Corrosion Science 217 (2023) 111124

Contents lists available at ScienceDirect

Corrosion Science

journal homepage: www.elsevier.com/locate/corsci

A general-purpose adsorption isotherm for improved estimation of standard adsorption free energy

Anton Kokalj

Department of Physical and Organic Chemistry, Jožef Stefan Institute, Jamova 39, SI-1000 Ljubljana, Slovenia

ARTICLE INFO

Keywords:
Standard adsorption free energy
Adsorption isotherms
Corrosion inhibitors

ABSTRACT

A new general-purpose Type–I adsorption isotherm is proposed to improve standard adsorption Gibbs energy estimation. This new isotherm stems from considering a functional dependence of various adsorption models on the c/θ vs. c plot, where θ is the fractional surface coverage and c the concentration. It can accurately describe many adsorption isotherms, implying that it is flexible enough to describe various adsorption scenarios. Among the tested adsorption models that the new isotherm can describe are those that consider lateral inter-adsorbate interactions, molecular size, surface heterogeneity, and mobile adsorption.

1. Introduction

In corrosion inhibition studies, the standard adsorption Gibbs energy ($\Delta G^{\circ}_{\mathrm{ads}}$) is often estimated via the linear regression of the $c/\theta = 1/K + mc$ equation, where c is the inhibitor concentration in the bulk solution, θ is the inhibitor fractional surface coverage, K is the adsorption equilibrium constant, and the m is the slope of the line on the c/θ vs. c plot. This equation originates from the Langmuir adsorption isotherm, which in the c/θ form reads $c/\theta = 1/K + c$. The difference between the two is in the slope m, which, for the Langmuir adsorption isotherm, is 1. In the previous publication [2], the $c/\theta = 1/K + mc$ equation was scrutinized conceptually, and it was demonstrated to be an effective equation that can decently describe various adsorption models. This observation explains why so many studies found that the equation can fit their experimental data. It was further shown that any significant deviation from the slope of 1 signals non-Langmuir adsorption due to inter-adsorbate interactions, multi-site adsorption, or surface heterogeneity.

Based on the insight gained in the previous publication [2], a new empirical general-purpose Type–I adsorption isotherm is proposed herein (for the classification of adsorption isotherm types, see, for example, Ref. [3]). This new isotherm stems from considering a functional dependence of various adsorption models on the c/θ vs. c plot. It is demonstrated that the new empirical isotherm can fit different Type–I adsorption isotherms (eleven different isotherms were tested), implying that it is flexible enough to describe various adsorption scenarios. The new isotherm can therefore be used to provide an improved estimate of the standard adsorption Gibbs energy from the experimentally determined surface coverages at different solute concentrations. However, an isotherm can provide an accurate estimate of the standard adsorption Gibbs energy only when surface coverages are reliably determined experimentally. In corrosion inhibition literature, corrosion inhibition efficiency (η) is usually used as a proxy for fractional surface coverage[1]. This practice was recently criticized by Lindsay et al. [4] by showing that the $\theta \approx \eta$ assumption is not necessarily valid. For this reason, we will consider the $\theta \neq \eta$ case in the subsequent publication [5] and develop a model where surface coverage depends on inhibition efficiency through a functional dependence.

2. Results and discussion

The analysis of the c/θ dependence on c for various isotherms reveals that for Type–I isotherms for which the saturation coverage is normalized to 1, c/θ eventually becomes linearly proportional to c with the slope of 1 at high concentrations [2][2]. In contrast, at very low concentrations, the slope (m_0) can deviate considerably from 1 and depends on the adsorption isotherm type. However, the slope usually changes very gradually from m_0 at low coverage to 1 at high coverage,

E-mail address: tone.kokalj@ijs.si.
URL: http://www.ijs.si/ijsw/K3-en/Kokalj.

[1] The $\theta \approx \eta$ assumption implies that the more exergonic the $\Delta G^{\circ}_{\mathrm{ads}}$ value, the more efficient the corrosion inhibitor is. However, this implication is not necessarily true because a sound argument can be made that a stronger molecule–surface bonding does not yet entail a better corrosion inhibition. For a conceptual discussion of this issue, see section 3.4 of Ref. [1].

[2] For a given solute, a saturation (monolayer) coverage may require concentration beyond the saturation concentration. In such a case, a hypothetical auxiliary solute that is equivalent to the real solute but displays an unlimited solubility can be envisaged.

https://doi.org/10.1016/j.corsci.2023.111124
Received 22 December 2022; Received in revised form 17 March 2023; Accepted 21 March 2023
Available online 28 March 2023

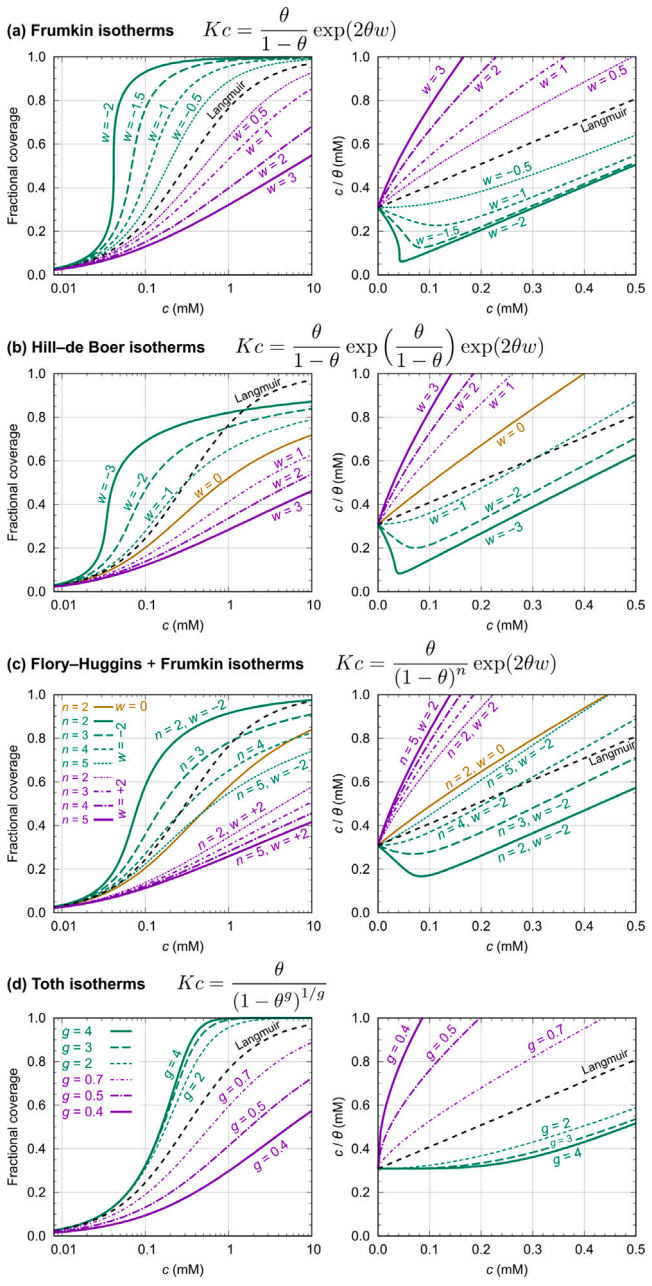

Fig. 1. Four different types of adsorption isotherms that display significant deviation from linearity at low concentrations on the c/θ vs. c plot (right column). The left column shows the adsorption isotherm on the θ vs. c plots (the c axis is logarithmic). Note that the isotherms that appear above the Langmuir adsorption isotherm on the θ vs. c plots appear below the Langmuir adsorption isotherm on the c/θ vs. c plots and display a higher deviation from linearity.

which is why many studies found the linear $c/\theta = 1/K + mc$ ansatz to be useful for fitting. This ansatz corresponds to the following isotherm:

$$Kc = \frac{\theta}{1-m\theta}. \tag{1}$$

It is evident that for $m > 1$, the equation is valid only for small coverages because, for $\theta > m^{-1}$, the denominator is negative, implying a negative concentration (or equilibrium constant), which is meaningless. It was shown in the preceding study [2] that this equation corresponds to a low coverage approximation of the Flory–Huggins type isotherm, i.e.:

$$Kc = \frac{\theta}{(1-\theta)^m} \approx \frac{\theta}{1-m\theta} \qquad \text{for } \theta \ll 1. \tag{2}$$

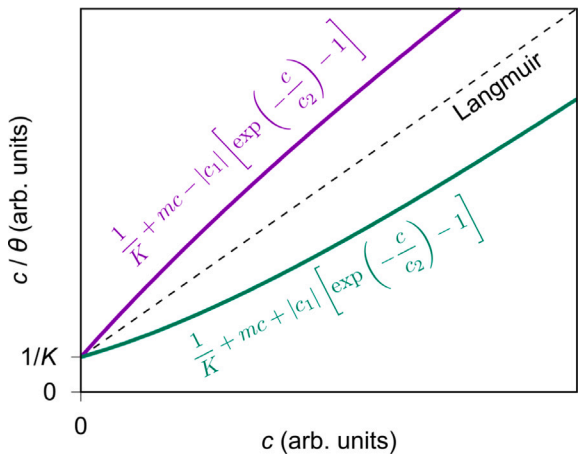

Fig. 2. A schematic behavior of the new empirical adsorption isotherm on the c/θ vs. c plot. If the c_1 parameter is positive, the isotherm (green curve) appears below the Langmuir adsorption isotherm and vice-versa for the negative c_1 (purple curve). (For interpretation of the references to color in this figure legend, the reader is referred to the web version of this article.)

In some cases, particularly when interactions between adsorbates are attractive, the c/θ curve shows significant curvature at low concentrations. Fig. 1 shows several adsorption isotherms that display considerable deviation from linearity at low concentration on the c/θ vs. c plot. The shown isotherms are Frumkin [6], Hill–de Boer [7,8], Flory–Huggins [9,10], and Toth [11]; the corresponding isotherm equations are stated in the figure (for further info about these isotherms, see Table 1). In such cases, an even better estimate of the intercept can be achieved by replacing the equation:

$$\frac{c}{\theta} = \frac{1}{K} + mc \tag{3}$$

with:

$$\frac{c}{\theta} = \frac{1}{K} + g(c), \tag{4}$$

where $g(c)$ is a function of the concentration. The requirements for the function $g(c)$ are that it smoothly changes the slope from m_0 at $c = 0$ to 1 at $c \to \infty$. However, in practice, the fitting is performed over some range of concentrations, and at the highest utilized concentration ($c_{\max}$), the slope may not yet be close to 1. Hence, we allow for the slope to be adjustable. A function that fulfills these requirements is:

$$g(c) = mc + c_1\left[\exp\left(-\frac{c}{c_2}\right) - 1\right], \tag{5}$$

where m, c_1, and c_2 are fitting parameters (note that m is unitless, while c_1 and c_2 have a unit of concentration); $c_1 > 0$ when the slope increases and $c_1 < 0$ when the slope decreases with the increasing concentration c, see Fig. 2. In contrast, c_2 is constrained to be positive. For the nonlinear fit to succeed, the initial values for m, c_1, and c_2 should be reasonably chosen. Namely, a nonlinear fit is not guaranteed to converge to a global minimum because it can be trapped in a local minimum. Reasonable starting values (within an order of magnitude from the optimal solution) improve the chances of finding a good solution. A decent choice of initial values is $m = 1$ with $|c_1| = c_2$ set to some value between the lowest ($c_{\min}$) and highest ($c_{\max}$) utilized concentrations. Usually, $|c_1| = c_2 = c_{\max}$ works fine, but if it fails, then a concentration (c_0) where the deviation from linearity appears on the c/θ vs. c plot can be used instead[3]. The rationale behind this choice is that the exponential term aims to describe this nonlinearity; with this

[3] In some problematic cases, it further helps to substitute m and c_2 with $|m|$ and $|c_2|$ in Eq. (5) to require explicitly m and c_2 to be positive.

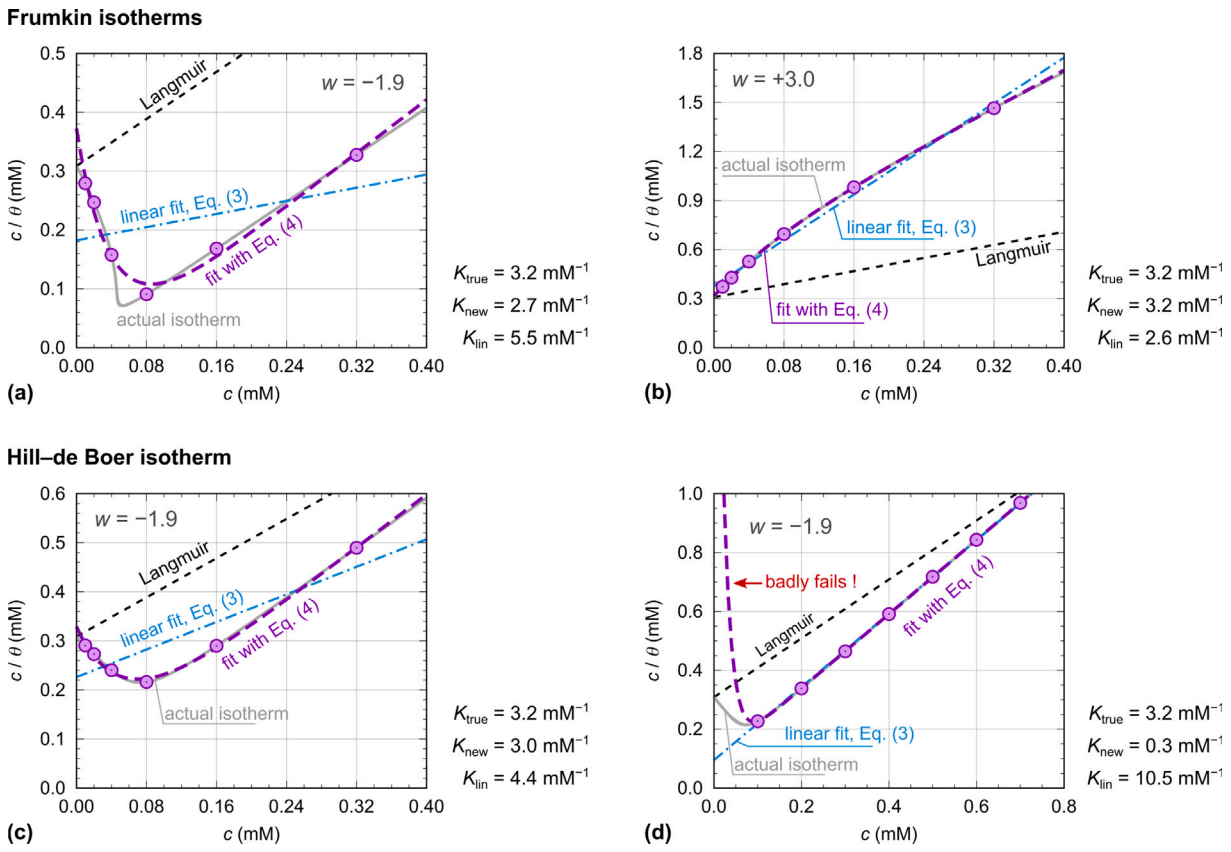

Fig. 3. Data points generated at several different concentrations with the (a, b) Frumkin and (c, d) Hill–de Boer adsorption isotherms (for the corresponding isotherm equations, see Table 1). The actual isotherms are shown with gray curves, and their approximations obtained by fitting the data points with the new isotherm of Eq. (4) are shown with purple dashed curves. The blue dash–dotted lines show the linear regressions of Eq. (3). The equilibrium constants obtained by fitting the data points with the new isotherm (K_{new}) and the linear regression (K_{lin}) are compared to the true equilibrium constant (K_{true}), corresponding to $\Delta G^{\circ}_{\text{ads}} = -30$ kJ/mol at room temperature, cf. Eq. (8). The black dashed line shows the Langmuir isotherm corresponding to the K_{true} value. (For interpretation of the references to color in this figure legend, the reader is referred to the web version of this article.)

choice, the magnitude of the derivative of the exponential term at c_0 is $|(\partial c_1 \exp(-c/c_2)/\partial c)_{c=c_0}| = e^{-1}$, implying that for $c > c_0$, the "influence" of the exponential term quickly becomes marginal.

It should be noted that adsorption equilibrium constant K can be estimated from the c/θ vs. c plot, via Eq. (3) or (4), only for cases that are asymptotically linear at low c, implying that the $\lim_{c\to 0} Kc \propto \theta$ relation holds. An example of the isotherm that is not linear at low c is the Langmuir–Freundlich isotherm [12,13]:

$$Kc = \frac{\theta^g}{(1-\theta)^g}, \qquad \text{hence for} \begin{cases} g < 1: & \lim\limits_{c\to 0} \dfrac{c}{\theta} = \infty \\ g > 1: & \lim\limits_{c\to 0} \dfrac{c}{\theta} = 0. \end{cases} \tag{6}$$

The performance of Eq. (4) with $g(c)$ represented by Eq. (5) was tested for several tens of cases using "virtual" experiments, where data points were generated with the adsorption isotherms considered in Fig. 1 at different sets of concentrations. The sets differ in concentration ranges and the distribution of concentrations within the set (either linear or logarithmic). The so-generated data points were then fitted by Eq. (4) with $g(c)$ represented by Eq. (5). Fitting was performed with the Gnuplot software [23], using the nonlinear least-squares Marquardt–Levenberg algorithm [24,25]. Some notable examples are shown in Fig. 3 in the form of the c/θ vs. c plots. It was found that the new method can well describe almost all tested cases. However, it may fail for close-to-linear cases, where the linear equation can be used instead. More specifically, it is not that Eq. (5) fails (a perfectly linear case is represented by Eq. (5) with $c_1 = 0$ so that $g(c) = mc$) but rather a fit fails due to unfortunate choice of data points; cases, where fit fails, can easily be spotted visually.

Fig. 3a shows attractive Frumkin isotherm (gray curve) for $w = -1.9$, which is close to the phase-transition that appears for $w < -2$, where adsorbates condense on the surface. This isotherm is an example of a notable deviation from the linearity at a low concentration that cannot be decently described by the linear regression of Eq. (3). In contrast, the new method performs quite well. Fig. 3b shows the case of a repulsive Frumkin isotherm ($w = +3$); here, the deviation from the linearity is much smaller, and the linear regression is good enough, yet the new method is still superior.

The example generated with an attractive Hill–de Boer isotherm is shown in Fig. 3c (for $w = -1.9$). Here the deviation from linearity is considerable, and the new method fits the data points almost perfectly (the isotherm and the fitted curve are superposed). The same isotherm is considered in Fig. 3d, but the data points are chosen in the linear region at higher concentrations. This is an example where the fitting with the new method fails, i.e., it "explodes" at low concentration leading to an order of magnitude overestimated intercept (the reason is that the first point is slightly above the line, while other points are perfectly linear). Such cases are easily detectable by visual inspection. The equilibrium constants K, obtained with the linear regression and the new method, are also presented in Fig. 3. The new method provides better estimations than the linear regression, except for the already discussed linear case of Fig. 3d.

The finding that Eq. (4) with $g(c)$ represented by Eq. (5) is able to describe various Type–I isotherms, suggests a new empirical general-purpose isotherm:

$$\theta = \frac{c}{\dfrac{1}{K} + mc + c_1\left[\exp\left(-\dfrac{c}{c_2}\right) - 1\right]}, \tag{7}$$

Table 1
Summary of various adsorption isotherms that were used to test the new isotherm of Eq. (7) in Fig. 4. The isotherms are written in the $Kc = f(\theta)$ form, and those that are linear at low c are normalized to give the K^{-1} intercept on the c/θ vs. c plot (the normalization factor $\mathcal{N}$ is explicitly written for cases, where $\mathcal{N} \neq 1$)[a].

Adsorption isotherm	Equation	Linear at low c	Takes into account
isotherms without the Frumkin term			
(a) Flory–Huggins[†] type [9,10]	$Kc = \frac{\theta}{(1-\theta)^n}$	yes	molecular size (substitutional adsorption)
(b) Bockris–Swinkels[‡] [14]	$Kc = \mathcal{N}\frac{\theta}{(1-\theta)^n}\frac{(\theta + n(1-\theta))^{n-1}}{n^n}, \quad \mathcal{N} = n$	yes	molecular size (substitutional adsorption)
(c) Temkin[§] [15]	$Kc = \mathcal{N}\frac{1-e^{-f\theta}}{e^{-f\theta}-e^{-f}}, \quad \mathcal{N} = \frac{1-e^{-f}}{f}$	yes	surface heterogeneity
(d) Toth [11]	$Kc = \frac{\theta}{(1-\theta^g)^{1/g}}$	yes	surface heterogeneity
(e) Langmuir–Freundlich (Sips) [12,16]	$Kc = \frac{\theta^g}{(1-\theta)^g}$	no	surface heterogeneity
isotherms with the Frumkin $\exp(2w\theta)$ *term*			
(f) Frumkin (Fowler–Guggenheim) [6]	$Kc = \frac{\theta}{1-\theta}\exp(2w\theta)$	yes	lateral interactions
(g) Hill–de Boer [7,8]	$Kc = \frac{\theta}{1-\theta}\exp\left(\frac{\theta}{1-\theta}\right)\exp(2w\theta)$	yes	mobile adsorption + lateral interactions
(h) Helfand–Frisch–Lebowitz [17] + Frumkin [18]	$Kc = \frac{\theta}{1-\theta}\exp\left(\frac{\theta(3-2\theta)}{(1-\theta)^2}\right)\exp(2w\theta)$	yes	molecular size (hard spheres) + lateral interactions
(i) Flory–Huggins[†] type + Frumkin [19,20]	$Kc = \frac{\theta}{(1-\theta)^n}\exp(2w\theta)$	yes	molecular size (substitut. ads.) + lateral interactions
(j) Kastening–Holleck[†] [21,22]	$Kc = \frac{\theta}{(1-\theta)^n}(1-\theta+\frac{\theta}{n})^{n-1}\exp(2w\theta)$	yes	molecular size (substitut. ads.) + lateral interactions
(k) Temkin[§] [15] + Frumkin	$Kc = \mathcal{N}\frac{1-e^{-f\theta}}{e^{-f\theta}-e^{-f}}\exp(2w\theta), \quad \mathcal{N} = \frac{1-e^{-f}}{f}$	yes	surface heterogeneity + lateral interactions

[a] Description of parameters:
$n \equiv$ parameter accounting for relative molecular size in substitutional adsorption, i.e., $\mathrm{Mol}_{(sol)} + n\mathrm{H_2O}_{(ads)} \rightleftharpoons \mathrm{Mol}_{(ads)} + n\mathrm{H_2O}_{(sol)}$.
$f \equiv$ parameter describing surface heterogeneity ($f \geq 0$).
$g \equiv$ parameter describing surface heterogeneity (typically, $0 < g \leq 1$ for the Toth isotherm and $g \geq 1$ for the Langmuir–Freundlich isotherm).
$w \equiv$ parameter describing lateral interactions ($w < 0$ for attraction and $w > 0$ for repulsion); note that the Frumkin term is often written with the opposite sign convention as $\exp(-2w\theta)$ or even without the factor 2 as $\exp(-w\theta)$.
[†] For the Flory–Huggins type isotherm, the simple $\theta/(1-\theta)^n$ form is used because it gives the K^{-1} intercept on the c/θ vs. c plot [2].
[‡] The normalization factor $\mathcal{N} = n$ is used so that the isotherm gives the K^{-1} intercept on the c/θ vs. c plot.
[§] The normalization factor $\mathcal{N} = (1-e^{-f})/f$ is used so that the isotherm gives the K^{-1} intercept on the c/θ vs. c plot [2].

where m, c_1, and c_2 are the empirical parameters described above. For the isotherm to be applicable over the whole coverage (or concentration) range, m should be close to 1. The reason is that coverage increases with increasing concentration until eventually a full monolayer coverage is reached, $\theta \approx 1$. From this point on, $c/\theta \approx c/1 = c$, which implies the slope of 1 on the c/θ vs. c plot. But the slope of 1 corresponds to $m = 1$.

The performance of the new empirical adsorption isotherm of Eq. (7) was tested on eleven different Type–I adsorption isotherms; these isotherms are specified in Table 1. To this end, the standard adsorption Gibbs energy (ΔG°_{ads}) of −30 kJ/mol was chosen[4] and the adsorption equilibrium constant was calculated for $T = 298.15$ K using the relation:

$$K = \frac{1}{c_{H_2O}}\exp\left(-\frac{\Delta G^{\circ}_{ads}}{RT}\right), \tag{8}$$

where c_{H_2O} is the molar concentration of liquid water (55.34 M at 25 °C)[5]. The $1/c_{H_2O}$ factor stems from considering the aqueous-phase adsorption as substitutional adsorption where an inhibitor molecule replaces a water molecule on the surface (for details, see Ref. [2]). For each of these isotherms, from six to eight different variants were considered by scanning the isotherm's parameters but keeping the constant K fixed to the value described above. In particular, the n parameter of the Flory–Huggins term and the Temkin heterogeneity parameter f were scanned from 1 to 7. The Frumkin lateral interaction parameter w ranged from $[-3, 3]$. As to widen the range of possibilities, for the Toth and Langmuir–Freundlich adsorption isotherms, both the $0 < g \leq 1$ and $g > 1$ ranges were probed, although usually, for the Toth isotherm, g ranges from 0 to 1 and, for the Langmuir–Freundlich isotherm, $g > 1$. These isotherms were fitted with the new isotherm in the concentration range from 0 to 10 mM. The fitting was performed in two different ways, i.e., in the $c/\theta = f(c)$ form by Eq. (4) and in the $\theta = f(c)$ form by Eq. (7), where $f(c)$ stands for a *function of a concentration*. The two variants are named as "c/θ–vs–c" and "θ–vs–c" in the following. The results of the "θ–vs–c" fitting are shown in Fig. 4, and the "c/θ–vs–c" fitting is presented in Fig. S1 in the Supplementary Material. Table 2 tabulates the ΔG°_{ads} values estimated with both fitting variants.

Among the considered adsorption isotherms, the new isotherm performs the worst for describing the Langmuir–Freundlich (LF) adsorption isotherm, which is not surprising because the LF isotherm is not linear at low concentrations, while the new isotherm is (this is also the reason that the LF isotherms cannot be fitted in the "c/θ–vs–c" form and are missing in Fig. S1). The "θ–vs–c" fitting also performs less satisfactorily for some isotherms that contain the Frumkin $\exp(2w\theta)$ term with significantly attractive interactions (i.e., $w \leq -1.9$), for which the predicted ΔG°_{ads} values are usually too endergonic. The analysis reveals that the reason for poor fits is the "explosion" at low concentrations, schematically presented in Fig. 3d. In contrast, the "c/θ–vs–c" fitting performs better for such "attractive" isotherms and predicts ΔG°_{ads} much more accurately (further analysis of one such specific case is presented in the next paragraph). To make the error analysis more apparent, Fig. 5 presents histograms of the relative

[4] This value corresponds to the order of magnitude of many reported ΔG°_{ads} values in the corrosion inhibition literature and is in between the threshold values of −20 and −40 kJ/mol that are often used to distinguish between physisorption and chemisorption. Note that this 20/40 rule was criticized recently [1] by arguing that it is not a reliable criterion to distinguish between the two adsorption modes.

[5] A value of 55.5 M is often used instead, corresponding to a density of water of 1 kg/L. But the correct density at 25 °C is 0.997048 kg/L [26].

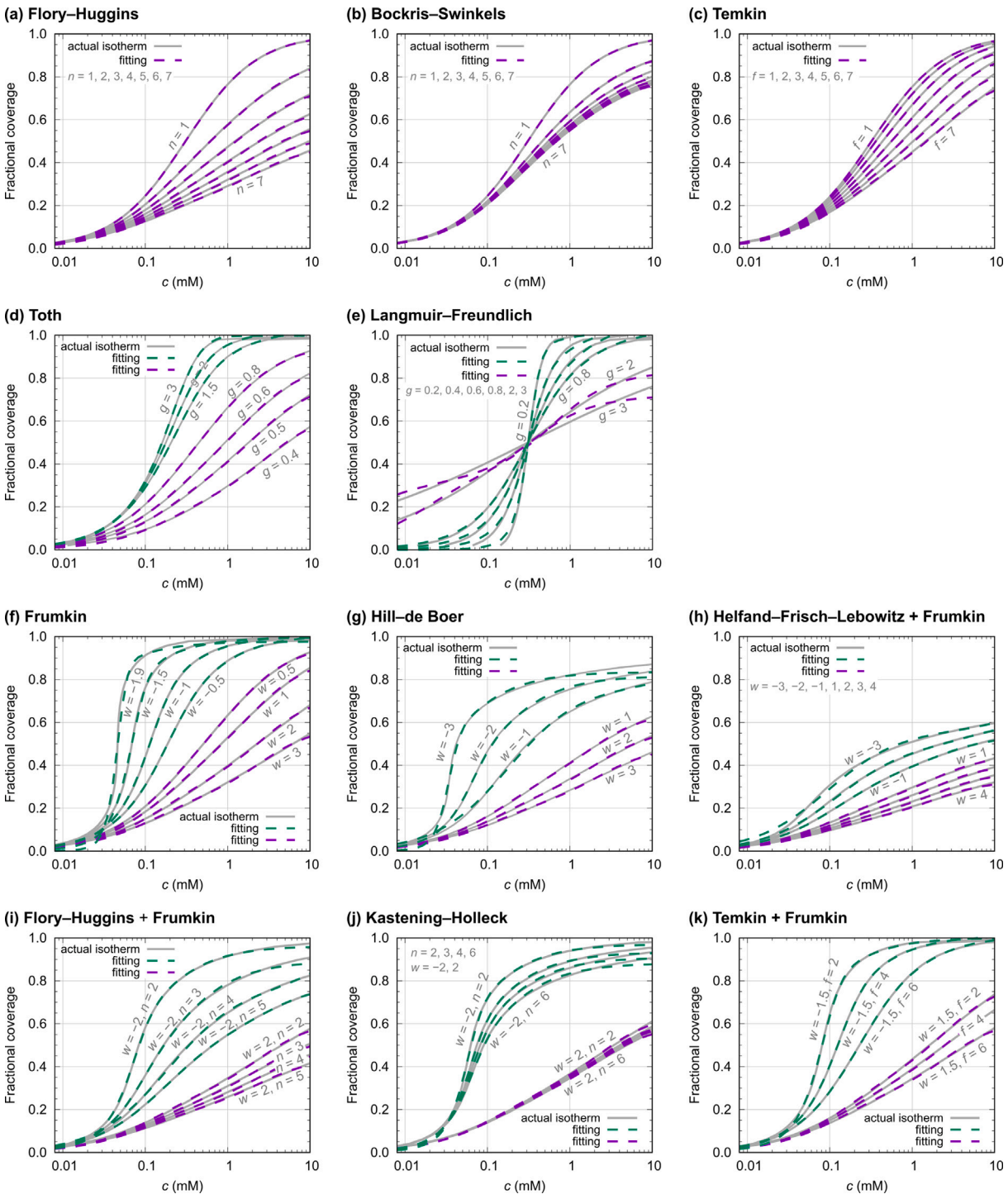

Fig. 4. Testing the performance of the new empirical adsorption isotherm of Eq. (7) (green and purple dashed curves) by fitting eleven different Type-I adsorption isotherms (gray curves behind the color dashed curves) that are specified in Table 1. Several different isotherms of each type are considered. (For interpretation of the references to color in this figure legend, the reader is referred to the web version of this article.)

error magnitudes in $\Delta G^{\circ}_{\mathrm{ads}}$. It is evident that the "c/θ–vs–c" fitting outperforms the "θ–vs–c" fitting in estimating the $\Delta G^{\circ}_{\mathrm{ads}}$ values. For the latter, of 77 examples, 25 (or 32%) have a relative error below 1%, and 3/4 of cases have an error within 3%. There are seven outliers with an error larger than 10%; four of them belong to the LF isotherms, and three of them to the isotherms that contain the Frumkin term with significantly attractive interactions. In contrast, there are no outliers for the "c/θ–vs–c" fitting (note that the non-linear LF isotherms are excluded), where 45% of examples have the relative error within 1% and about 90% of cases have the error within 3%. The highest relative error is 7%.

Both fitting forms require a nonlinear fit, which, as commented above, is not guaranteed to converge to a global minimum. For most of the considered cases, both forms give compatible results (cf. Figs. 4 and S1 and Table 2). However, differences emerge for "difficult" cases, where the "c/θ–vs–c" fitting outperforms the "θ–vs–c" fitting

Table 2
Estimated ΔG°_{ads} values by fitting the eleven isotherm types shown in Fig. 4 with the newly proposed isotherm. The data are presented as "*isotherm parameters: θ–vs–c fitted* ΔG°_{ads} (*c/θ–vs–c fitted* ΔG°_{ads})", where "θ–vs–c" means that θ was fitted by Eq. (7) as $\theta = f(c)$, whereas the "c/θ–vs–c" fitting was performed with Eq. (4) as $c/\theta \propto g(c)$; the latter ΔG°_{ads} values are written in parentheses. The true ΔG°_{ads} value is −30.0 kJ/mol. There are seven "θ–vs–c" ΔG°_{ads} estimates with relative error magnitudes greater than 10%; these outliers are written in red. In contrast, there are no "c/θ–vs–c" ΔG°_{ads} outliers. The Langmuir–Freundlich (LF) isotherms cannot be "c/θ–vs–c" fitted because the LF isotherms are not linear at small coverage.

Flory–Huggins	Bockris–Swinkels	Temkin	Toth	Langmuir–Freundlich	Frumkin
$n = 1$: −30.0 (−30.0)	$n = 1$: −30.0 (−30.0)	$f = 1$: −30.0 (−30.0)	$g = 3.0$: −29.8 (−29.9)	$g = 3.0$: −38.5 (/)	$w = 3.0$: −29.2 (−29.3)
$n = 2$: −29.8 (−29.8)	$n = 2$: −29.9 (−29.9)	$f = 2$: −30.0 (−30.0)	$g = 2.0$: −30.0 (−30.0)	$g = 2.0$: −34.7 (/)	$w = 2.0$: −29.3 (−29.4)
$n = 3$: −29.7 (−29.7)	$n = 3$: −29.9 (−29.9)	$f = 3$: −29.9 (−29.9)	$g = 1.5$: −30.1 (−30.1)	$g = 0.8$: −28.8 (/)	$w = 1.0$: −29.6 (−29.7)
$n = 4$: −29.6 (−29.6)	$n = 4$: −29.9 (−29.9)	$f = 4$: −29.8 (−29.8)	$g = 0.8$: −29.7 (−29.8)	$g = 0.6$: −27.1 (/)	$w = 0.5$: −29.8 (−29.9)
$n = 5$: −29.4 (−29.4)	$n = 5$: −29.9 (−29.9)	$f = 5$: −29.7 (−29.7)	$g = 0.6$: −29.1 (−29.3)	$g = 0.4$: −24.8 (/)	$w = -0.5$: −30.0 (−30.0)
$n = 6$: −29.4 (−29.3)	$n = 6$: −29.9 (−29.9)	$f = 6$: −29.6 (−29.6)	$g = 0.5$: −28.6 (−28.8)	$g = 0.2$: −19.5 (/)	$w = -1.0$: −29.4 (−29.9)
$n = 7$: −29.3 (−29.2)	$n = 7$: −29.9 (−29.9)	$f = 7$: −29.5 (−29.6)	$g = 0.4$: −27.7 (−28.0)		$w = -1.5$: −27.0 (−29.7)
					$w = -1.9$: −20.1 (−29.5)

Hill–de Boer	Helfand–Frisch–Lebowitz + Frumkin	Flory–Huggins + Frumkin	Kastening–Holleck	Temkin + Frumkin
w=3.0: −29.2 (−29.6)	w=4.0: −29.1 (−29.0)	w=2.0, n=2: −29.3 (−29.3)	w=2.0, n=2: −29.3 (−29.4)	w=1.5, f=2: −29.4 (−29.4)
w=2.0: −29.3 (−29.4)	w=3.0: −29.2 (−29.0)	w=2.0, n=3: −29.2 (−29.2)	w=2.0, n=3: −29.3 (−29.4)	w=1.5, f=4: −29.3 (−29.3)
w=1.0: −29.6 (−29.6)	w=2.0: −29.3 (−29.2)	w=2.0, n=4: −29.2 (−29.1)	w=2.0, n=4: −29.3 (−29.4)	w=1.5, f=6: −29.2 (−29.2)
w=−1.0: −30.7 (−30.6)	w=1.0: −29.5 (−29.4)	w=2.0, n=5: −29.1 (−29.0)	w=2.0, n=6: −29.3 (−29.4)	w=−1.5, f=2: −28.2 (−29.6)
w=−2.0: −28.9 (−31.8)	w=−1.0: −30.1 (−30.0)	w=−2.0, n=2: −28.6 (−29.6)	w=−2.0, n=2: −26.7 (−29.7)	w=−1.5, f=4: −29.7 (−29.9)
w=−3.0: −22.1 (−29.6)	w=−2.0: −30.6 (−30.5)	w=−2.0, n=3: −29.6 (−31.2)	w=−2.0, n=3: −28.0 (−29.7)	w=−1.5, f=6: −30.2 (−30.1)
	w=−3.0: −31.5 (−31.3)	w=−2.0, n=4: −30.6 (−30.5)	w=−2.0, n=4: −28.3 (−29.8)	
		w=−2.0, n=5: −30.2 (−30.1)	w=−2.0, n=6: −28.6 (−29.8)	

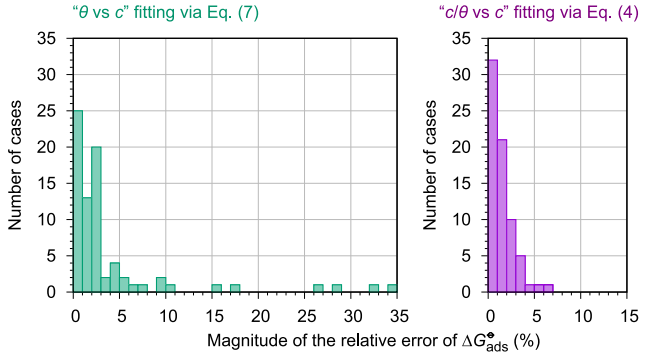

Fig. 5. Histograms of the relative error magnitudes in the estimated ΔG°_{ads} values by fitting the isotherms shown in Fig. 4 with the newly proposed isotherm, i.e., the histograms are built from the data in Table 2. The left histogram (green) shows the ΔG°_{ads} errors of the "θ–vs–c" fitting with Eq. (7), and the right histogram (purple) presents the errors of the "c/θ–vs–c" fitting with Eq. (4). (For interpretation of the references to color in this figure legend, the reader is referred to the web version of this article.)

in estimating ΔG°_{ads} and also yields easier fit convergence[6]. For the considered cases, the "c/θ–vs–c" fits quickly converged using the proposed initial values of $m = 1$ and $|c_1| = c_2 = c_{max}$, with the initial value of K set to 10^3. In contrast, the "θ–vs–c" fits required more iterations (e.g., in three cases several thousand iterations were required for convergence). One difficult case (an "attractive" Frumkin isotherm with $w = -1.9$), where the two fits give different results is presented in Fig. 6. While the "c/θ–vs–c" fit accurately predicts the ΔG°_{ads} value (−29.5 kJ/mol to be compared to the true value of −30.0 kJ/mol), the "θ–vs–c" fit gives a poor estimate of −20.1 kJ/mol. The reason for the poor performance is the "explosion" as the concentration approaches zero (green dot–dashed curve in Fig. 6b). This explosion leads to a considerably overestimated $1/K$ intercept and, consequently, a much too low value of the equilibrium constant. In contrast, the "c/θ–vs–c" fit gives a rather accurate description at small concentrations (purple dashed curve in Fig. 6b). However, the "c/θ–vs–c" fit is not without problems. Fig. 6a reveals that it gives a nonphysical description at intermediate coverages between 0.1 and 1 mM, where it displays a bogus maximum, while the "θ–vs–c" fit is well behaved. Based on this analysis, we can conclude that the "c/θ–vs–c" fitting is better suited for estimating ΔG°_{ads} values and describing coverage dependence at low concentrations, whereas the "θ–vs–c" fitting is more reliable at higher concentrations.

[6] A tight convergence threshold was used for fitting, i.e., the Gnuplot's `FIT_LIMIT` variable was set to 10^{-7} (the default value is 10^{-5}).

3. Conclusions

A new general-purpose Type–I adsorption isotherm was proposed by considering a functional dependence of various adsorption models on the c/θ vs. c plot. Such plots are often utilized in corrosion inhibition studies, where the standard adsorption Gibbs energy (ΔG°_{ads}) is usually estimated via the linear regression using the $c/\theta = 1/K + mc$ equation. In particular, by linearly extrapolating the experimental data to $c = 0$, the inverse of the adsorption equilibrium constant is obtained from which ΔG°_{ads} is calculated. While this equation was often found to represent the experimental data well—the reasons for its success were explained in the preceding study [2]—in some cases, particularly when interactions between adsorbates are significantly attractive, the c/θ curve shows significant curvature at low concentrations. In such cases, the linear regression does not perform well, while the proposed isotherm reasonably describes the nonlinearity and provides a superior estimation of the equilibrium adsorption constant and, consequently, ΔG°_{ads}. The new isotherm replaces the linear mc term with the flexible $mc + c_1[\exp(-c/c_2) - 1]$ ansatz, where m, c_1, and c_2 are empirical parameters.

Although the idea for the new isotherm emerged in the context of corrosion inhibitors, it is not limited by them. Instead, it generally applies to molecular adsorption from either the gas or solvent phase due to its ability to accurately describe various adsorption scenarios, including those that involve inter-adsorbate interactions, molecular size, surface heterogeneity, and mobile adsorption. The only limitation is that it is targeted at describing up to a complete monolayer coverage.

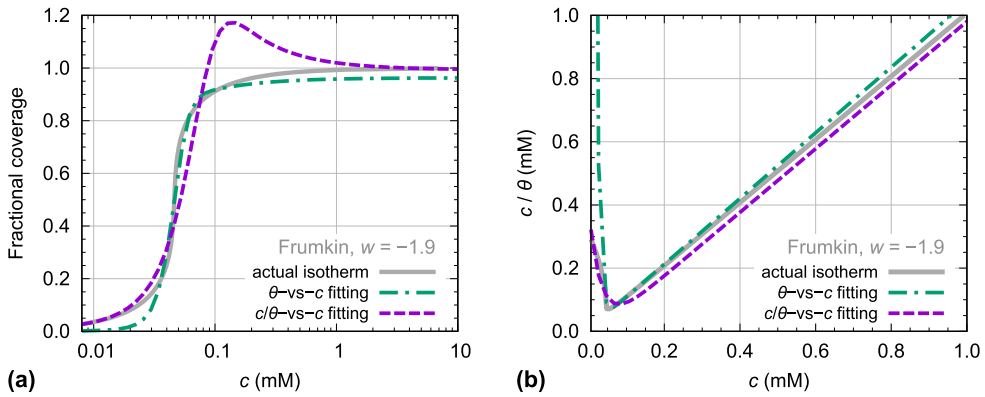

Fig. 6. Approximating the "attractive" ($w = -1.9$) Frumkin isotherm (solid gray curve) with the new isotherm by using either the "θ–vs–c" fitting with Eq. (7) (green dash–dotted curve) or the "c/θ–vs–c" fitting with Eq. (4) (purple dashed curve). In (a), the three isotherms are shown on the θ vs. c plot, and in (b), on the c/θ vs. c plot. (For interpretation of the references to color in this figure legend, the reader is referred to the web version of this article.)

CRediT authorship contribution statement

Anton Kokalj: Conceptualization, Methodology, Investigation, Formal analysis, Writing – original draft, Writing – review & editing, Visualization.

Declaration of competing interest

The author declares that he has no known competing financial interests or personal relationships that could have appeared to influence the work reported in this paper.

Data availability

The data used by the manuscript are contained within it, whereas the scripts used for fitting and generating the graphs will be made available on request

Acknowledgments

This work has been financially supported by the Slovenian Research Agency (Grant No. P2-0393).

Appendix A. Supplementary data

Supplementary material related to this article can be found online at https://doi.org/10.1016/j.corsci.2023.111124.

References

[1] A. Kokalj, Corrosion inhibitors: physisorbed or chemisorbed? Corros. Sci. 196 (2022) (2021) 109939, http://dx.doi.org/10.1016/j.corsci.2021.109939.
[2] A. Kokalj, On the use of the Langmuir and other adsorption isotherms in corrosion inhibition, Corros. Sci. 217 (2023) 111112, http://dx.doi.org/10.1016/j.corsci.2023.111112.
[3] K.S.W. Sing, Reporting physisorption data for gas/solid systems with special reference to the determination of surface area and porosity (recommendations 1984), Pure Appl. Chem. 57 (4) (1985) 603–619, http://dx.doi.org/10.1351/pac198557040603.
[4] M.S. Walczak, P. Morales-Gil, R. Lindsay, Determining Gibbs energies of adsorption from corrosion inhibition efficiencies: Is it a reliable approach? Corros. Sci. 155 (2019) 182–185, http://dx.doi.org/10.1016/j.corsci.2019.04.040.
[5] A. Kokalj, On the estimation of standard adsorption free energy from corrosion inhibition efficiencies, Corros. Sci. 217 (2023) 111139, http://dx.doi.org/10.1016/j.corsci.2023.111139.
[6] A. Frumkin, Die kapillarkurve der höheren fettsäuren und die zustandsgleichung der oberflächenschicht, Z. Phys. Chem. 116U (1) (1925) 466–484, http://dx.doi.org/10.1515/zpch-1925-11629.
[7] T.L. Hill, Statistical mechanics of multimolecular adsorption II. Localized and mobile adsorption and absorption, J. Chem. Phys. 14 (7) (1946) 441–453, http://dx.doi.org/10.1063/1.1724166.
[8] J.H. de Boer, The Dynamical Character of Adsorption, Oxford University Press, Oxford, 1953.
[9] J.O. Bockris, A.K.N. Reddy, M. Gamboa-Aldeco, Modern Electrochemistry, Vol. 2A, second ed., Kluwer Academic/Plenum Publishers, New York, Boston, Dordrecht, London, Moscow, 2000.
[10] H.P. Dhar, B.E. Conway, K.M. Joshi, On the form of adsorption isotherms for substitutional adsorption of molecules of different sizes, Electrochim. Acta 18 (11) (1973) 789–798, http://dx.doi.org/10.1016/0013-4686(73)85030-3.
[11] W. Rudziński, S. Sokolowski, M. Jaroniec, J. Tóth, Analytical approximations for multilayer adsorption isotherms in adsorption systems yelding the Dubinin-Radushkevich and the Tóth adsorption isotherms in submonolayer coverage region, Z. Phys. Chem. 256 (1) (1975) 273–284, http://dx.doi.org/10.1515/zpch-1975-25636.
[12] R. Sips, On the structure of a catalyst surface, J. Chem. Phys. 16 (5) (1948) 490–495, http://dx.doi.org/10.1063/1.1746922.
[13] N. Ayawei, A.N. Ebelegi, D. Wankasi, Modelling and interpretation of adsorption isotherms, J. Chem. 2017 (2017) 3039817, http://dx.doi.org/10.1155/2017/3039817.
[14] J.O'M. Bockris, D.A.J. Swinkels, Adsorption of n-decylamine on solid metal electrodes, J. Electrochem. Soc. 111 (6) (1964) 736, http://dx.doi.org/10.1149/1.2426222.
[15] M.I. Temkin, The kinetics of some industrial heterogeneous catalytic reactions, in: Adv. Catal. 28, Academic Press, Cambridge, MA, USA, 1979, pp. 173–291, http://dx.doi.org/10.1016/S0360-0564(08)60135-2.
[16] D.G. Kinniburgh, General purpose adsorption isotherms, Environ. Sci. Technol. 20 (1986) 895–904, http://dx.doi.org/10.1021/es00151a008.
[17] E. Helfand, H.L. Frisch, J.L. Lebowitz, Theory of the two- and one-dimensional rigid sphere fluids, J. Chem. Phys. 34 (3) (1961) 1037–1042, http://dx.doi.org/10.1063/1.1731629.
[18] I.B. Ivanov, K.P. Ananthapadmanabhan, A. Lips, Adsorption and structure of the adsorbed layer of ionic surfactants, Adv. Colloid Interface Sci. 123-126 (2006) 189–212, http://dx.doi.org/10.1016/j.cis.2006.05.020.
[19] R. Parsons, The electrical variable and the form of the isotherm for the adsorption of organic compounds at electrodes, J. Electroanal. Chem. 8 (2) (1964) 93–98, http://dx.doi.org/10.1016/0022-0728(64)87002-9, 1959-1966.
[20] J. Lawrence, R. Parsons, Adsorption isotherms in mixed solvent systems, J. Phys. Chem. 73 (11) (1969) 3577–3581, http://dx.doi.org/10.1021/j100845a008.
[21] B. Kastening, L. Holleck, Die bedeutung der adsorption in der polarographie, Talanta 12 (12) (1965) 1259–1288, http://dx.doi.org/10.1016/0039-9140(65)80229-6.
[22] D.M. Bastidas, R.R. Gómez, E. Cano Díaz, The isotherm slope: A criterion for studying the adsorption mechanism of benzotriazole on copper in sulphuric acid, Rev. Metal. Madrid 41 (2) (2005) 98–106, http://dx.doi.org/10.3989/revmetalm.2005.v41.i2.192.
[23] T. Williams, C. Kelley, et al., Gnuplot 5.4, 2020, http://www.gnuplot.info/.
[24] K. Levenberg, A method for the solution of certain non-linear problems in least squares, Q. Appl. Math. 2 (2) (1944) 164–168, http://dx.doi.org/10.1090/qam/10666.
[25] D.W. Marquardt, An algorithm for least-squares estimation of nonlinear parameters, J. Soc. Ind. Appl. Math. 11 (2) (1963) 431–441, http://dx.doi.org/10.1137/0111030.
[26] D.R. Lide, CRC Handbook of Chemistry and Physics, eighty fifth ed., CRC Press, Boca Raton, Florida USA, 2005.